ELSEVIER

Journal of Molecular Catalysis A: Chemical 162 (2000) 147–157

JOURNAL OF MOLECULAR CATALYSIS A: CHEMICAL

www.elsevier.com/locate/molcata

The importance of acid site locations for *n*-butene skeletal isomerization on ferrierite

L. Domokos [a], L. Lefferts [a], K. Seshan [a], J.A. Lercher [b,*]

[a] *Catalytic Processes and Materials, Faculty of Chemical Technology, University of Twente, P.O. Box 217, 7500 AE, The Netherlands*
[b] *Technische Universität München, Institut für Technische Chemie, D-85749 Garching, Germany*

Dedicated to Prof. H. Knözinger on the occasion of his 65th birthday.

Abstract

The role of the acid site location in H-ferrierite (H-FER) on the skeletal isomerization of linear butenes was studied. Assignment of OH groups observed in FTIR analysis is addressed taking into account previous NMR and computational studies regarding the FER structure. Possible locations of alkali ions in the zeolite framework are discussed. Close structure activity relationship has been observed between Brønsted acid sites located in the 10 member ring (MR) channels and selective isobutene formation. Molecular dynamics (MD) calculations of possible products observed during *n*-butene transformation at reaction temperatures support the experimental findings.

Keywords: Ion exchange; Butene isomerization; Ferrierite; Brønsted acidity

1. Introduction

Over the past decade, skeletal isomerization of linear butenes has been intensively investigated [1]. Catalysts based on (halogenated) alumina, silica, silica–alumina and related materials were reported to have limited lifetime during butene isomerization [2,3]. Substantial coke formation and butene dimerization were observed with these catalysts [4]. In many cases, water has been cofed to increase catalyst lifetime and isobutene selectivity.

Medium pore zeolites, however, show remarkable performance allowing yields of isobutene close to the thermodynamic limits even under severe operating conditions [5–9]. At partial pressures of *n*-butene close to 1 bar and relatively low temperatures, where oligomerization of olefins is a favored side reaction of skeletal isomerization, it was possible to achieve close to 50 mol% yield of isobutene at 350°C in a single pass over H-ferrierite (H-FER) [10]. Other type of medium pores zeolites such as TON, AEL were also reported to be good catalysts for this reaction [11–13]. In contrast to TON and AEL, FER contains a two-dimensional pore system, where 8 and 10 member ring (MR) channels are perpendicularly interconnected. Although it was early realized that pore dimensions are crucial, it is unclear to present, whether or not the additional eight MR channels (side channels) in FER contribute to the selective isomerization reaction [14].

It has been thoroughly demonstrated that skeletal isomerization of linear butene is catalyzed by Brønsted acid sites [15]. It was also shown that

* Corresponding author. Tel.: +49-89-289-13540; fax: +49-89-289-13544.
E-mail address: johannes.lercher@ch.tum.de (J.A. Lercher).

1381-1169/00/$ - see front matter
PII: S1381-1169(00)00286-7

Lewis sites do not have a significant influence on the selective reaction, although they might promote side reactions, such as hydride transfer. Thus, the role of Brønsted acid sites distribution on the overall catalytic performance has to be explored in detail to obtain a fundamental understanding of the elementary steps in *n*-butene skeletal isomerization.

Although the structure of FER is well established [16], the possible location and distribution of acid sites in the framework is still debated. Several methods were applied in order to differentiate between their locations. Based on theoretical calculations, it has been proposed that Brønsted acid sites in the 10 MR channels would be favored for sites in the eight MR channels [17,18]. Sarv et al. [19] using ^{23}Na, ^{27}Al and ^{29}Si solid state NMR showed that Na^+ ions are preferably located in the eight MR channels of FER, while Brønsted acid sites are located in the 10 MR channels. Thus, in a partially ion-exchanged HFER strong Brønsted acidic hydroxyl groups are preferentially located in the 10 MR channels, while Na^+ would be mostly located in the eight MR channels [19].

Potassium-exchanged FER showed similar trends [20]. Neutron diffraction showed that K^+ ions were located preferentially in the side channels, although the distribution of potassium was different compared to sodium. The size of the K^+ ion did not allow its extensive packing in the side channels as in the case of sodium, more K^+ ions were located in the main (10 MR) channel of FER.

Using infrared (IR) spectroscopy, molecular modeling and kinetic analysis of butene isomerization reaction, this paper aims at demonstrating how the catalytic activity of acid sites in the 10 and 8 MR channels in partially exchanged H-FER can be attributed to their location. Implications on the structure–activity relation using results obtained will be outlined.

2. Experimental

2.1. Catalyst preparation

FER sample was obtained from Tosoh with a nominal Si/Al ratio of 8 in Na/K form. Si/Al ratio of 8.1 was reconfirmed by SEM-EDX. The catalyst was transformed into its ammonium form by successive ion exchange with 1 M NH_4NO_3 solution at room temperature. The particle size was measured with scanning electron microscopy and platelet-like particles with a diameter of 1 μm and a cross-section of 0.05 μm were observed. BET surface area of the sample was 202 m^2/g with an apparent micropore surface area of 165 m^2/g.

Total acid site concentration determined by temperature programmed desorption (TPD) with NH_4^+ exchanges samples (liquid ion exchange) was 2.05 mmol/g. A single desorption peak of ammonia was observed between 250°C and 450°C. ^{27}Al MAS NMR did not show the presence of extra framework aluminum in the parent sample. Using pyridine adsorption, Al^{3+} induced Lewis acid sites were not detected in an in situ activated sample (for more details see Ref. [21]).

For preparing partially ion-exchanged FER, the concentration of NH_4NO_3 was varied and the procedure was performed in one step with the parent catalyst in order to gain low ammonium content. The samples were successively washed with deionized water and dried at room temperature in air. The chemical composition determined by XRF analysis is compiled in Table 1.

2.2. TPD

TPD was carried out in vacuo using a temperature increment of 10°C/min in the range of 150–700°C. In a typical experiment, 45–50 mg of the sample were evacuated to the base pressure of the system (10^{-2} Pa) at 150°C for 60 min to desorb the majority of physisorbed molecules and heated to 700°C with

Table 1
Chemical composition of ion-exchanged samples in wt.% determined by XRF analysis

Samples	Composition (mol%)				
	Al	Si	Na	K	Si/Al
H-FER-100	10.8	89.1	0.0	0.1	8.2
H-FER-65	10.6	86.8	0.1	2.6	8.2
H-FER-30	9.9	81.5	0.4	8.1	8.2
H-FER-16	9.8	80.0	0.9	9.3	8.2
H-FER-7	9.7	79.3	1.4	9.5	8.2
Parent material	9.6	79.0	1.9	9.6	8.2

10°C/min. The desorption curves obtained were normalized to the weight of the samples. The reactor was a quartz glass tube connected with a vacuum pump and a quadrupole mass spectrometer (Balzers QMG 420) for detection of the desorbed species.

2.3. IR spectroscopy

The activation of partially ion-exchanged samples was monitored in a vacuum IR cell, which was placed in a BRUKER VECTOR22 IR spectrometer. The stainless steel cell with CaF_2 windows was evacuated to a base pressure of 10^{-6} mbar. The samples were pressed into self-supporting wafers of approximately 3 mg/cm^2 and activated in situ at 500°C. Spectra presented here are recorded at 350°C in transmission absorption mode. Detailed information on the experimental procedures can be found in Refs. [22,23].

2.4. Catalytic measurements

The catalytic tests were conducted in a tubular continuous flow system equipped with quartz reactor. All measurements were carried out with 20 mg of zeolite catalyst at temperature range of 250–450°C with total pressure between 1.1 and 1.3 bars. The catalyst without binder was held by quartz wool plugs in the isothermal part of the oven. During reaction a feed of 10 vol.% 1-butene (Scott Specialty Gases, 99%) in argon (Praxair, 5.0) was used. The weight hourly space velocity of butene was varied in order to obtain conversions of 1-butene below 10 mol%.

The catalyst was activated in situ in the reactor in dry argon (99.995%) flow of 60 ml/min with a ramp of 2°/min to 400°C. The temperature was maintained for 1 h at 400°C and subsequently lowered to reaction temperature. Then, the pure Ar flow was switched to a mixture of 1-butene and Ar. More details of the procedure during kinetic analysis can be found in Ref. [24].

The effluent stream was analyzed on-line by gas chromatography using a 50-m HP-PLOT/Al203 column ("S" deactivated). Data was analyzed by Chromatography Station for Windows (DataApex version 1.7). Initial rates are taken from 3 min time on stream over a fresh catalyst. Carbon balance was close to 98% throughout the experiments.

2.5. Forced molecular dynamics (MD)

Calculations were performed on a Silicon Indigo^2 workstation running Insight II program package from MSI using the Discover, Solids Builder and Solids Diffusion modules. These calculations allowed a constant directional external force to be imposed on a guest molecule in a zeolite framework during an MD calculation. Guest molecules were diffused in the direction of the force along the 10 and 8 MR channels of FER. The MD calculations were performed at 623 K using the Discover package. Molecular interactions between the hydrocarbon molecules and the zeolite pore were calculated with the cff91 czeo force field. Displacement of 0.5 Å with 4000 dynamic steps (real time simulation of 4000 fs) ensured multiple passes of molecules into channel intersections and pore openings with good reproducibility in the energy profiles. During simulation, molecular conformations were stored periodically to an archive file for analysis. The stored conformations including the overall energy of the cluster were used to calculate the average energy barrier for diffusion in and out from cages present in FER.

3. Results

3.1. TPD

The TPD profiles of ammonia from liquid phase ion-exchanged FER samples are given in Fig. 1. Annotation of the samples is based on the relative acid site concentration (Table 2). NaH-FER-65, therefore, denotes as a sample containing 65% of the total exchange sites in acidic form and 35% of the sites exchanged with alkali ions. During TPD a single peak of desorbing ammonia between 200°C and 450°C was observed. Repeating the experiment on a preactivated sample (activated at 400°C for 1 h in vacuum) with subsequent ammonia adsorption at room temperature and evacuation at 150°C for 1 h resulted in the same TPD spectrum indicating that only the decomposition of NH_4^+ contributed to both experiments.

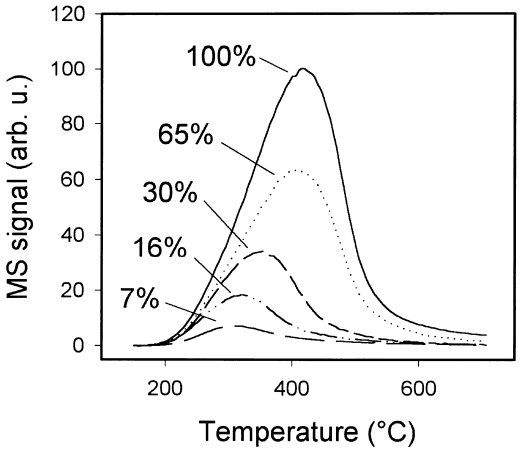

Fig. 1. TPD of ammonia after liquid ion-exchanged at room temperature. Parent material: Na-FER with Si/Al ratio of 8, evacuation at 150°C for 1 h prior to experiment.

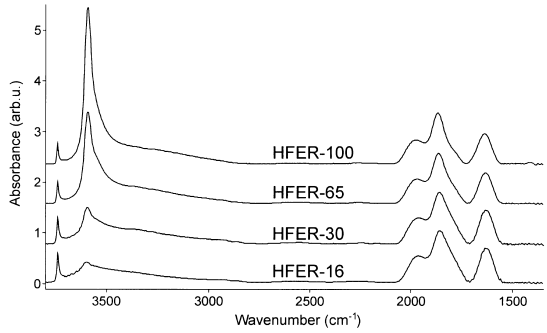

Fig. 2. In situ IR spectra of activated partially ion-exchanged H-FER samples. Notation is based on the integrated TPD curves of ammonia desorption. Spectra recorded at 350°C in vacuum (base pressure of 10^{-6} mbar) after activation at 500°C for 1 h.

3.2. IR spectroscopy

The values of acid site concentration obtained from TPD were in good agreement with the integrated areas assigned to the Brønsted acid sites at 3593 cm^{-1} acquired using in situ IR spectroscopy (Table 2). The band corresponding to the terminal OH groups (silanol groups) was found at 3741 cm^{-1} (Fig. 2). The overtones of the lattice vibrations were found in the region of 2500–1550 cm^{-1}.

As it was reported earlier [25–27], the main peak has an asymmetric shape, being extended to lower frequencies with a less pronounced shoulder at 3550 cm^{-1}. In order to evaluate the possible contribution of acid sites at different location in the FER structure to this complex peak, a deconvolution procedure was performed on the experimental spectra. Curve fitting of the spectra using a set previously proposed by Ref. [28] did not give satisfactory results. Although a good fit could be obtained over the fully acidic sample, with decreasing acid site concentration the relative intensities of the peaks did not reflect the expected qualitative change in acid site location demonstrated by NMR.

Modification of the position and width of peaks used resulted in full convergence at different acid site concentrations (Fig. 3) with less peaks and minimal solutions in residuals. The first three bands at 3743, 3601 and 3591 cm^{-1} are assigned to the terminal OH, the bridging OH located in the 10 MR channels, and in the cages in the eight MR channels, respectively. The fourth peak at 3561 cm^{-1} is tentatively assigned to the Brønsted acid sites in the six

Table 2
Acid site concentration determined by TPD of ammonia and IR spectroscopy over partially ion-exchanged samples

Sample	Acid site concentration		
	Relative (%)		Absolute (mmol/g)
	From temperature programmed desorption	From infrared	From temperature programmed desorption
H-FER-100	100	100	2.05
H-FER-65	65	69	1.33
H-FER-30	30	25	0.61
H-FER-16	16	15	0.33
H-FER-7	7	8	0.14

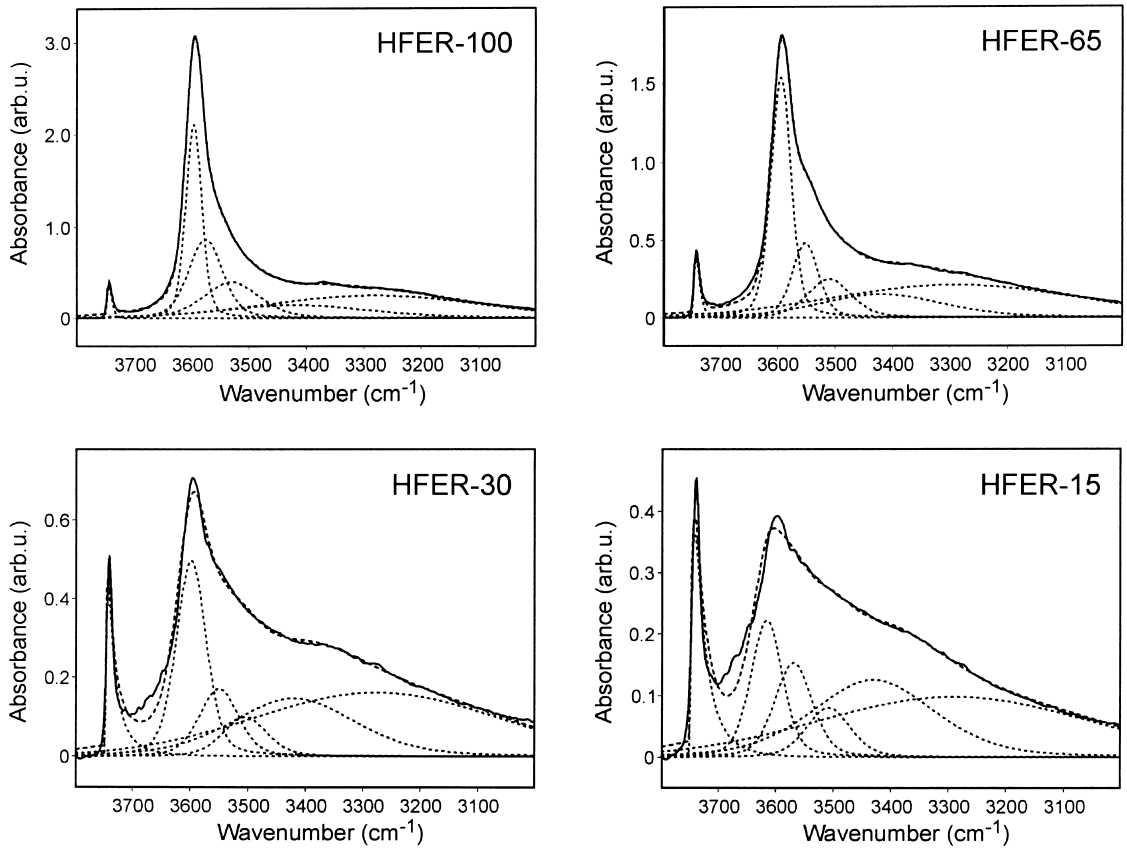

Fig. 3. Deconvolution of IR spectra of partially ion-exchanged samples.

MRs, pointing towards the 10 MR channels [20]. The assignment of the remaining two bands are ambiguous, the fifth band at 3540 cm^{-1} could be attributed to the OH groups in the five MRs [29].

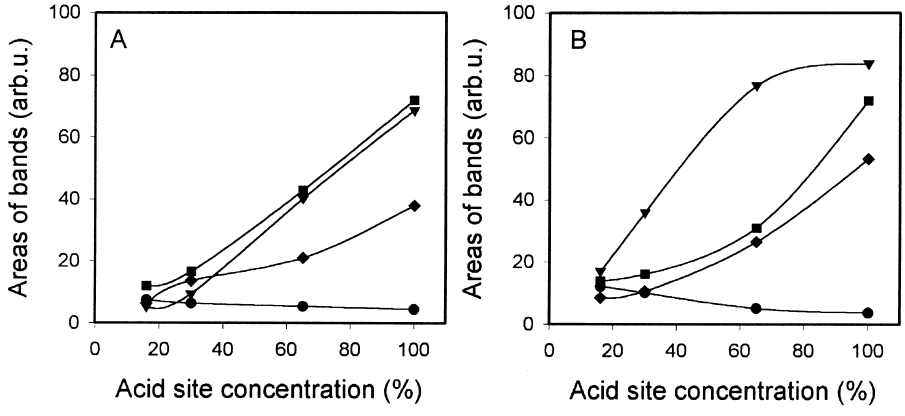

Fig. 4. Areas of deconvoluted bands from Fig. 3 in a function of acid sites concentration determined by ammonia TPD. Plot A: curve fit based on Zholobenko et al. [28]. Plot B: modified set of curve fit used, shown in Fig. 3. Legends: ● terminal OH groups, ▼ Brønsted acid sites in the 10 MR channels, ■ Brønsted acid sites in the eight MR channels, ◆ Brønsted acid sites in the six MR channels.

Comparison of the relative areas of fitted bands is graphically represented in Fig. 4. All the molar extinction coefficients of the deconvoluted peaks were assumed to be equivalent. This implies a uniform relation between the concentrations of sites to peak abundance contrary to what can be expected from the different properties (peak position and half width) of the corresponding bands. Nevertheless, it still provides a good indication of the variation in the relative concentration of different type of acid sites with increasing overall acid site concentrations.

The relative areas of different OH groups obtained from the deconvolution according to Ref. [28] are shown in Fig. 4A. Although wide fitting parameters were kept during deconvolution, only low acceptance in the convergence criteria could be achieved on samples with low Brønsted acid site concentrations. A linear decrease in intensity with decreasing overall acid site concentration can be observed for all OH groups. When the deconvolution was carried out with the modified set of parameters (Fig. 4B), the OH group assigned to the 10 MR channels shows saturation above 65% overall acid site concentration in line with expectations from ^{29}Si and ^{27}Al MAS NMR [19]. Similar discrepancy from the linearity is not observed with the other OH groups.

3.3. Catalytic performance

The rates of formations of ethene, propene, isobutene and pentenes in the function of acid site concentration are presented in Fig. 5. As it can be seen, the rate of propene, pentene and ethene forma-

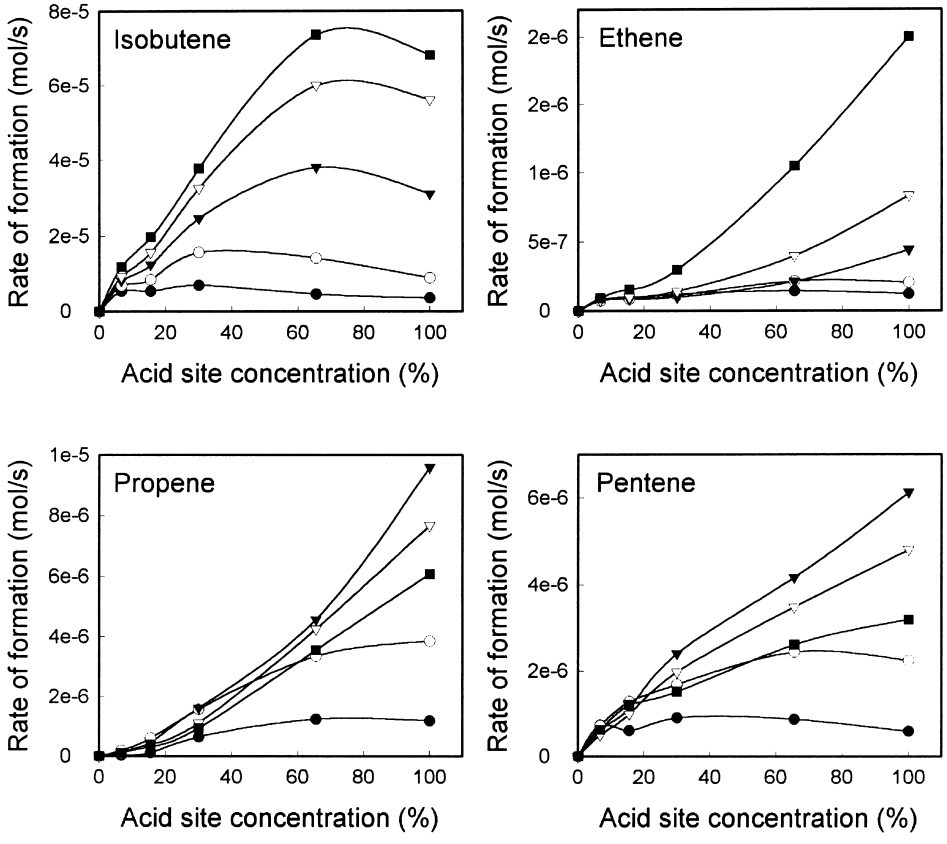

Fig. 5. Initial rate of formation of isobutene, ethene, propene and pentenes as the function of acid site concentration. Data collected at 3 min TOS at various temperatures with 1-butene pressure of 100 mbar and WHSV of 160 h^{-1}. Legends: ● 250°C, ○ 300°C, ▼ 350°C, ▽ 400°C, ■ 450°C.

tion is a linear function of acid site concentration in a wide range of temperatures over FER. However, the rate of isobutene formation reached its maximum at approximately 65% of acid sites. Further increase in acid site concentration did not improve the isobutene production in the whole temperature range. At lower temperatures (below 350°C), the maximum was reached at already 30% of acid sites available. This shows that for an optimum concentration of isobutene, not all the acid sites are required in the pore structure. Oligomerization and subsequent cracking resulting in propene and pentenes, on the other hand, were further enhanced by increasing acid site concentration at all the temperatures.

3.4. Molecular modeling

The average energy barrier, the lowest energy and the position of the molecule in the framework obtained at 350°C during forced MD of selected molecules are given in Table 3. The calculations were performed in the direction of the 8 or 10 MR channels in order to estimate the threshold a molecule has to pass while entering or leaving a channel. Since in the direction of the side channels 8 and 10 member cages are alternating, a separate number was obtained for entering or leaving an eight MR cage for every molecule. This allows to detach diffusion barriers in this direction, when molecules are formed inside of the cage or forced to enter it.

In the direction of the 10 MR ring channels, all linear molecules showed very low energy barriers during forced diffusion except *cis*-2-butene. The barrier *cis*-2-butene undergoes is much higher due to its nonlinear shape inducing large intermolecular repulsion during diffusion. As expected, the branched molecules exhibit higher energy barriers in the 10 MR channels compare to the linear structures. Isobutene and 2-methyl-2-butene showed relatively smaller barrier compare to 2,2,4-trimethyl-pentane (2,2,4-TMP), which was above 100 kJ/mol. The variation of approximately 20 kJ/mol in the observed energy barriers is mainly due to the change in the conformation of the molecules passing through the pore. It should be noted that the calculations were performed at 350°C, which already induces several conformational isomers in larger molecules.

The diffusion pathway in the direction of the eight MR channels is more complicated. Since in FER

Table 3
Estimated diffusion properties of selected molecules in FER structure

Molecule	$E_{barrier}$ (kJ/mol)		
	8 Member ring		10 Member ring
	Entering the cage[a]	Leaving the cage[b]	Across the window
Ethene	8	9	−2[c]
Propene	20	29	4
1-Butene	71	80	10
trans-2-Butene	12	24	2
cis-2-Butene	59	59	48
Isobutene	250	360	30–50[d]
1-Pentene	75	103	17
trans-2-Pentene	64	100	6
2-Methyl-1-butene	160	140	58–80[d]
2-Methyl-2-butene	200	210	25–50[d]
2,2,4-TMP[e]	550	800	110

Forced MD were performed in the direction of the 8 and 10 MR channels at 623 K with rigid framework. Simulation time: 4000 fs. Numbers are taken after a periodic pattern in the energy profile was reached.

[a] Energy barrier when the molecule enters the eight MR cages from the 10 MR channels.

[b] Energy barrier when the molecule leaves the eight MR cages to the 10 MR channels.

[c] Stabilized at the window.

[d] Depending on the local conformation of molecule.

[e] 2,2,4-TMP.

alternating cages and 10 MR channels in the direction of the eight MR channels exist, diffusing guest molecules will undergo two different transitions. They can enter the eight MR cages only from the 10 MR channels, and they will leave the eight MR cages into a 10 MR channels.

Considerable higher diffusion barriers were found for linear and branched molecules in the direction of the eight MR channels. Branched molecules, such as isobutene, methylbutenes and 2,2,4-TMP showed remarkably high barrier (see Table 3) in entering or leaving the 8 member cages. It is interesting to note that that pentene isomers showed slightly lower barriers compared to isobutene.

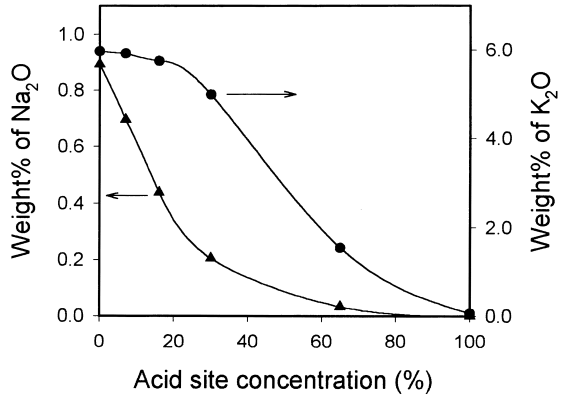

Fig. 6. Wt.% of sodium and potassium content of ion-exchanged samples in the function of acid site concentration. Circles correspond to K_2O, triangles to Na_2O content.

4. Discussion

Among the suitable zeolite catalysts for *n*-butene skeletal isomerization reaction, only FER has a two-dimensional pore system. Interestingly, FER is the only catalyst that was shown a significant variation in selectivity vs. time on stream. This raises the question whether the pore structure is related to the unusual catalytic behavior, and furthermore, if the arrangement and location of acid cites in FER have any effect on the catalytic performance.

Molecular modeling of the FER structure led to the conclusion that among the existing locations, acid sites are preferably formed in the 10 MR channels. Additionally, it was concluded that alkali cations prefer the exchange positions in the eight MRs due to higher stabilization offered by the smaller zeolite pore in these channels. The experimental findings of Sarv et al. [19] based on ^{23}Na, ^{27}Al and ^{29}Si showed that indeed Na^+ is located in the eight MR channels of partially ion-exchanged FER samples. Furthermore, it was shown before [20] that alkali ions located in the side channels block the transport of molecules.

When Na^+ ions are replaced by K^+ ions, a different distribution occurs regarding the location of ions due to the larger size of potassium. Aluminum was found to be evenly distributed among the T sites (our sample is the same as the FER studied by Sarv et al. [19] and Wichterlova et al. [26]). Due to the configuration of T sites in FER (Fig. 6 and Ref. [30]), it is expected that aluminum at the T1 and T5 sites is compensated from the 6 MRs by potassium. Aluminum at the other T sites, T2, T3 and T4 is compensated from the 10 MR channels, either by Na^+ or K^+ ions.

Quantitatively, it means that two thirds of the exchange sites, approximately 60–65%, are compensated from the 10 MR channels by potassium, and the rest is from the eight MR cages. Practically, a larger variation of acid site concentration can be achieved in the 10 MR channels, when potassium is present instead of sodium.

The potassium and sodium content of the ion-exchanged samples are compared in Fig. 7. In general, sodium is exchanged preferentially. Sodium is nearly completely removed at already 30% NH_4^+ exchange level, as it is most likely located in the 10 MR channels, while potassium is found to be more stabilized in the eight MR channels.

Thus, we concluded that at low acid site concentrations, acid sites are most probably located in the 10 MR channels, while the exchange positions in the eight MR channels are occupied by Na^+ or K^+ ions. With increasing exchange degree, all the sites in the 10 MR channels are transformed to acidic hydroxyl groups.

Deconvolution of the bands of the Brønsted acidic hydroxyl groups leads to an independent insight over the possible locations of acid sites in the framework [31,32]. The deconvolution produced results very similar to those obtained with solid state NMR and

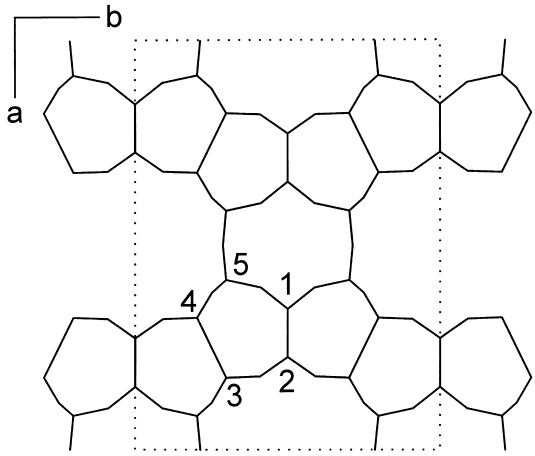

Fig. 7. FER framework projected on *ab* plane. Tetrahedral sites are numbered as in Ref. [30].

kinetic measurements (Fig. 3). Due to the different locations of alkali counter ions, the Brønsted OH groups assigned to the T4 sites cannot be differentiated from the other 10 MR channel acid sites, contrary to what has been suggested in Ref. [28]. Therefore, the three major Brønsted acidic peaks can be assigned directly to the bridging OH groups in the 10, 8 and 6 MR channels, respectively. The saturation observed in the abundance of the 10 MR channels OH groups at 65% of total acid site concentration (see Fig. 4) is in perfect agreement with the modeling studies, the kinetic results of this study and the NMR results of Sarv et al. [19].

When the relative abundance of the various Brønsted acid sites is compared to the rates of formation of different products (see Figs. 4 and 5), a remarkable similarity between isobutene formation and the abundance of acid sites in the 10 MR channels is observed. This strongly suggests that the rate of isobutene formation is a direct function of the Brønsted acid site concentration in the main channels. Since the presence of these acid sites in the eight MR channels did not increase the rate of isobutene formation, we conclude that the Brønsted acid sites in the side channels of FER do not play a significant role for this reaction.

Consecutive reactions starting from isobutene cannot be excluded in the fully acidic sample. The rate of isobutene formation reached its top at 65% of acid site concentration, and slightly decreased at 100%. This suggests that isobutene might have reacted further by for instance oligomerization and cracking leading to by-products over the acid sites in the eight MR channels. Nevertheless, it is clearly shown that acid sites in the eight MR channels do not improve the overall rate of isobutene formation in FER.

In contrast to isobutene, the formation of by-products, such as ethene, propene and pentene increased with increasing concentration of acid sites in the eight MR channels. The relative ease of diffusion of ethene and propene out of these channels supports this finding. Pentene formation is also improved by acid sites present in eight MR cages.

Based on data obtained from MD calculations, it was possible to estimate the average energy barrier a molecule has to overcome, when it migrates in the channels of FER at reaction temperatures. In general, under dynamic conditions linear molecules showed consistently lower diffusion barriers compared to branched ones. The slight increase in energy of the molecules containing a double bond at the end of the chain is mainly due to their less symmetric shape. The double bond at the end of the chain induced torsion in the structure during interaction with the pore wall. The same reasoning can explain the higher barrier for *cis*-2-butene as pointed out earlier.

In the direction of the eight MR channels, the differences between linear and branched molecules were plausibly larger. It is interesting to note that almost all of the molecules exhibited higher diffusion barrier leaving the eight MR cages compared to entering. Our observation showed that most of the molecules found very stable conformations in the eight MR cages. This can be attributed to the close interaction between the guests and the pore wall. Although the confined space allowed great stabilization, it also induced large repulsion with small displacements. This resulted in higher energy barriers during diffusion: the extensive repulsion forces brought significant torsion in the structure of hydrocarbon guests.

Under these circumstances, any additional stabilization can dramatically reduce the energy barrier. Indeed, pentenes showed somewhat lower energy barrier in diffusion in and out from these cages compare to isobutene, they were in the range of the linear butenes. Our calculations showed that when

these molecules were leaving the cage, significantly higher van der Waals attractive forces were present due to the extra carbon atom in their skeleton inducing further stabilization, and therefore reducing the overall barrier. Contrarily, in the case of the 2,2,4-TMP considerable relaxation in the cage was not observed. It can be rationalized as follows. First, the molecule did not stabilize in the cage because of the high repulsion forces present due to its bulkiness. In addition, the extensive branching of this molecule necessitated very high intramolecular torsion during diffusion resulting in extreme energy barriers.

Highly branched octenes, such as 2,2,4-TMP were proposed in the literature to be intermediates in butene isomerization. Our simulations showed that their formation is possible inside FER, but their diffusion is hindered in both the main and side channels. It implies that the adsorption of these types of molecules would be very difficult under reaction conditions, which is in excellent agreement with adsorption studies where branched octanes were found to have very low coverage [33]. Furthermore, it suggests that octenes involved in intracrystalline by-product or isobutene formation most probably rarely leave the zeolites particle if they are formed inside. This supports our previous finding, where kinetic data showed no correlation between octene, propene and pentene formation [24].

5. Conclusions

Using NH_4^+ liquid phase ion exchange of NaK-FER at ambient temperatures, it was possible to obtain FER samples with Brønsted acid sites exclusively in the 10 MR channels. The preferential adsorption of alkali ions made it possible to differentiate between acid sites located in the 10 and 8 MR channels (main channels and side channels, respectively). Comparison of the catalytic performance of samples having acid sites only in the main channels or in both main and side channels revealed that only the acid sites in the main channels are involved in the selective isomerization reaction leading to isobutene. Acid sites in the side channels (eight MR channels) are concluded to contribute to side reactions resulting in the formation of by-products, such as propene and pentenes. Thus, we conclude that only 10 MR channels are effective for *n*-butene skeletal isomerization, and the presence of additional eight MR pores does not improve the selectivity to isobutene. With respect to the fact that H-FER catalysts improve remarkably their selectivity to isobutene with time on stream, we speculate that in this process the acid sites in the eight MR cages deactivate.

Molecular modeling of alkanes in FER showed that the diffusion of highly branched hydrocarbons is somewhat hindered in the 10 MR channels. The diffusion barrier in the eight MR channels is, in contrast, so high for the same molecules that at reaction temperature directed motion cannot occur. In contrast, the energy barrier for monobranched pentenes was found to be in the range of butenes. This confirms the conclusions from experiments that the eight MR channels do not contribute to the selective isomerization reaction leading to isobutene, but might be involved in propene and pentene formation.

References

[1] I.E. Maxwell, J.E. Naber, K.P. de Jong, Appl. Catal., A 113 (1994) 153.
[2] V.R. Choudhary, Chem. Ind. Dev. 8 (1974) 31.
[3] Z-X. Cheng, V. Ponec, Appl. Catal., A 118 (1994) 127–138.
[4] J. Szabo, J. Perrotey, G. Szabo, J. Duchet, D. Cornet, J. Mol. Catal. 67 (1991) 79.
[5] US 5 491 276 assigned to Texaco Oil.
[6] EP 0 574 994 A1, EP 0 627 394 A1 assigned to Shell RTCA.
[7] US 5 321 194, PCT/US93/00766 assigned to Mobil Oil.
[8] EP 0 247 802 B1 assigned to BP.
[9] US 5 146 035 (UOP).
[10] H.H. Mooiweer, K.P. de Jong, B. Kraushaar-Czarnetzki, W.H.J. Stork, WB.C.H. Krutzen, Stud. Surf. Sci. Catal. 84 (1994) 2327.
[11] J. Houzvicka, S. Hansildaar, V. Ponec, J. Catal. 167 (1997) 273.
[12] R. Byggningsbacka, N. Kumar, L-E. Lindfors, J. Catal. 178 (1998) 611.
[13] L.H. Gielgens, I.H.E. Veenstra, V. Ponec, M.J. Haanepen, J.H.C. Hooff, Catal. Lett. 32 (1995) 195.
[14] P. Meriaudeau, C. Naccache, Adv. Catal. 44 (2000) 505.
[15] J. Houzvicka, V. Ponec, Appl. Catal., A 145 (1996) 95.
[16] W.M. Meier, D.H. Olson, Ch. Baerlocher, Atlas of Zeolite Structure Types, 4th edition, 1992.
[17] F. Blanco, G. Urbina-Villalba, M.M.R. de Agudelo, Mol. Simul. 14 (1994) 165.

[18] J. Jousse, L. Leherte, D.P. Vercauteren, Mol. Simul. 17 (1996) 175.
[19] P. Sarv, B. Wichterlova, J. Cejka, J. Phys. Chem. B 102 (1998) 1372.
[20] I.J. Pickering, P.J. Maddox, J.M. Thomas, A.K. Cheetham, J. Catal. 119 (1989) 261.
[21] J.A.Z. Pieterse, S. Veefking-Reyes, K. Seshan, L. Domokos, J.A. Lercher, J. Catal. 187 (1999) 518.
[22] F. Eder, J.A. Lercher, J. Phys. Chem. B 101 (1997) 1273.
[23] G. Eder-Mirth, Collect. Czech. Chem. Commun. 60 (1995) 421.
[24] L. Domokos, L. Lefferts, K. Seshan, J.A. Lercher, J. Catal. in press.
[25] M. Trombetta, G. Busca, S. Rossini, V. Piccoli, U. Cornaro, R. Guercio, R. Catani, R.J. Willey, J. Catal. 179 (1998) 581.
[26] B. Wichterlova, N. Zilkova, E. Uvarova, J. Cejka, P. Sarv, C. Paganini, J.A. Lercher, Appl. Catal., A 182 (1999) 297.
[27] E. Yoda, J.N. Kondo, F. Wakabayashi, K. Domen, Appl. Catal., A 194–195 (2000) 275.
[28] V.L. Zholobenko, D.B. Lukyanov, J. Dwyer, W.J. Smith, J. Chem. Phys. B 102 (1998) 2715.
[29] V.L. Zholobenko, L.M. Kustov, V.Yu. Borokov, V.B. Kazansky, Zeolites 8 (1988) 175.
[30] J.E. Lewis Jr., C.C. Freyhardt, M.E. Davis, J. Phys. Chem. 100 (1996) 5039.
[31] J.W. Ward, in: J.A. Rabo (Ed.), Washington, 1976, p. 118, Version 1.
[32] H. Karge, Stud. Surf. Sci. Catal. 65 (1991) 133.
[33] J. Houzvicka, PhD Thesis, University of Leiden, 1998.